

Thymol blue as corrosion inhibitor for carbon steel in 1 M hydrochloric acid solutions

Ameena Mohsen Al-Bonayan

Department of Chemistry, Faculty of Applied Science Girls, Umm Al-Qura University, Makkah Al-Mukarramah, Kingdom of Saudi Arabia, email: benayana@hotmail.com, Tel:00966125606179

Abstract: Corrosion inhibition of carbon steel in 1 M HCl by thymol blue was investigated using weight loss, potentiodynamic polarization, electrochemical impedance spectroscopy (EIS) and electrochemical frequency modulation (EFM) techniques. The results indicate that this compound inhibited the corrosion process in the medium by virtue of adsorption and inhibition efficiency improved with increasing its concentration. Inhibition mechanism was deduced from the temperature dependence of the inhibition efficiency as well as from activation parameters that govern the process. Polarization results revealed that thymol blue acts as mixed type inhibitor. Adsorption of thymol blue on the carbon steel was found to obey the Langmuir adsorption isotherm. The phenomenon of physical adsorption is proposed from the obtained thermodynamic parameters. The surface of C-steel was examined by both scanning electron microscopy (SEM) and energy dispersive X-ray (EDX).

[Ameena Mohsen Al-Bonayan. **Thymol blue as corrosion inhibitor for carbon steel in 1 M hydrochloric acid solutions.** *Nat Sci* 2015;13(4):106-115]. (ISSN: 1545-0740). <http://www.sciencepub.net/nature>. 16

Key words: Carbon steel, polarization, EIS, EFM, acid inhibition, Thymol blue

1. Introduction

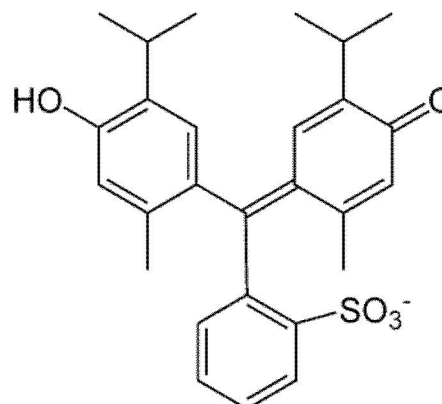
C-steel is a widely use alloy around the world. Although it is good properties and relatively cheap coast, it has a low resistance toward corrosion. Corrosion is considered to be one of the most annoying problems which affect the economy, environment and safety. One of the most famous techniques that uses to prevent corrosion is the usage of the organic inhibitors, a lot of studies carried out to study the corrosion inhibition using organic compounds[1-6]. Organic compounds specially that contains oxygen, sulfur and nitrogen elements have a great tendency toward inhibition of corrosion and widely used in industrial acid cleaning, acid de-scaling, acid pickling and oil well acidizing in order to restrain the corrosion attack on metallic materials[7-11]. Usually the inhibition mechanism for those compounds is by displacing water molecules on the surface and forming a compact barrier film via physisorption mechanism [12], The presence of no bonded (one pair) and π - electrons in alkenes, alkynes and aromatic rings in inhibitors may involve in chemisorption and the strength of the bond is depending on electron density and polarization of the donor atom of the functional group[13].

2. Experimental Method

2.1. Materials, chemicals and solutions

All experiments were running with carbon steel metal which it is chemical composition (weight %):0.200 C, 0.350 Mn, 0.024P, 0.003 S, and the remainder Fe. Corrosive solution (1 M HCl) solution was prepared by dilution of analytical grade (37%) HCl with bidistilled water. Stock solutions (10^{-3} M) of thymol blue were prepared by dissolving an

accurately weighed quantity of it in an appropriate volume of water, and then the required concentrations range (5×10^{-6} to 15×10^{-6}) were prepared by dilution with bidistilled water.



4-[9-(4-hydroxy-2-methyl-5-propan-2-yl-phenyl)-7,7-dioxo-8-oxa-7 λ 6-thiabicyclo [4.3.0] nona-1,3,5-trien-9-yl]-5-methyl-2-propan-2-yl-phenol (Thymol blue) Molecular formula $C_{27}H_{30}O_5S$, Molecular weight 466.59 g/mol

2.2. Weight loss measurements

Weight loss measurements were carried out at various temperature (25 to 50°C) for 3 hours, using a seven carbon steel coupons with rectangular form (2.5 x 2 x 0.2 cm) and 0.3 cm diameter hole for mounting by a glass rod. C-steel coupons were treated with emery paper (grades 320, 800 and 1200) to give a mirror-like surface, then washed with bidistilled water and acetone[14], after getting it's accurate weight in dry condition, C-steel coupons

were immersed in 100ml beaker contains 100 ml HCl with and without the additional of different concentrations of Thymol blue. After the specified periods of time, the specimen were taken out of the test solution, rinsed with bidistilled water, dried as before and weighed again accurately. The average weight loss at a certain time for each set of the seven samples was taken. The weight loss was recorded to nearest 0.0001g. Inhibition efficiency was calculated from the following relations [15]

$$\%IE = \theta \times 100 = [1 - (W/W^{\circ})] \times 100 \quad (1)$$

Where W° and W are the weight losses in the absence and presence of inhibitor, respectively.

2.3 Electrochemical techniques

Electrochemical measurements, including potentiodynamic polarization, (EIS) and EFM were performed in a three-electrode cell at room temperature (25°C). The counter electrode is a platinum electrode, the reference electrode is saturated calomel electrode (SCE) coupled to a fine Luggin capillary and the working electrode is prepared from C-steel as a square specimen sealed with epoxy (PTFE) to give a surface area of 1cm².

Electrochemical measurements were performed by using Gamry (PCI 300/4) instrument Potentiostat / Galvanostat/ZRA which includes a Gamry frame work system based on ESA400. Gamry applications include DC 105 for corrosion measurements and EIS 300 for electro chemical impedance spectroscopy and EFM 140 software along with a computer for collecting data, EChem analyst 5.58 software was used for plotting, graphing and fitting data.

3. Results and Discussion

3.1 Weight loss measurements

Figure (1) shows the weight loss-time curves for C-steel in 1M HCl in the absence and presence of different concentrations of the Thymol blue at 25°C. It is obvious that the weight loss of carbon steel in the presence of Thymol blue varies linearly with time, and is much lower than that obtained in blank solution. The linearity obtained indicated the absence of insoluble surface film during corrosion and that the Thymol blue was first adsorbed onto the metal surface and, therefore, impede the corrosion process [16]. The inhibition efficiency (%IE) and the surface coverage (θ) were calculated using equation (1) Table (1) shows the inhibition efficiency (% IE) and surface coverage value (θ) obtained at 25°C for the investigated Thymol blue. The data of Table (1) indicated that the inhibition efficiency increases with increasing the Thymol blue concentration. This behavior could be attributed to increase of the number of adsorbed molecules at metal surface [17].

3.2 Potentiodynamic polarization measurements

Before each Tafel experiment, the carbon steel electrode was allowed to corrode freely and its open circuit potential (OCP) was recorded as a function of time up to 30 min at potential of -1.5 V in order to reduce the pre-immersion oxide film covered the surface of the electrode. After this time a steady-state OCP, corresponding to the corrosion potential (E_{corr}) of the working electrode, was obtained. The potentiodynamic Tafel measurements were started from cathodic to the anodic direction, $E = E_{corr} \pm 250$ mV_{SCE}, with a scan rate of 1 mVs⁻¹. To calculate the efficiency stern Geary method [18] was applied to calculate corrosion current by extrapolation of anodic and cathode Tafel lines to a point which gives Log i_{corr} and the corresponding corrosion potential (E_{corr}) for the blank and in presence of different concentrations of the Thymol blue. Inhibition efficiency (%IE) and degree of surface coverage (θ) can be determined using equation (2) [19-20]:

$$\%IE = \theta \times 100 = [1 - (i_{corr(inh)} / i_{corr(free)})] \times 100 \quad (2)$$

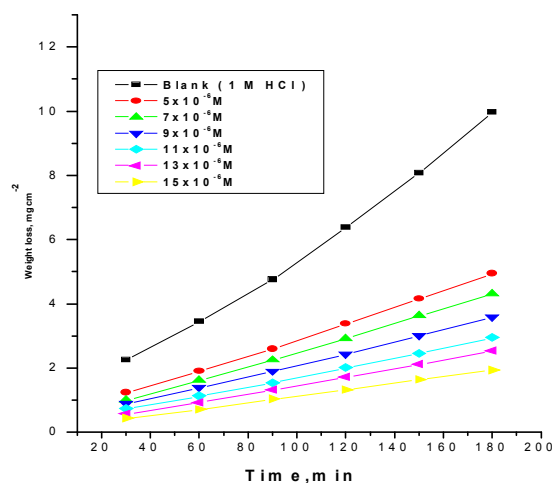


Figure 1. Weight loss-time curves for the corrosion of C-steel in 1 M HCl in the absence and presence of different concentrations of thymol blue at 25°C

Table (1): Surface coverage (θ) and inhibition efficiency (%IE) at different concentrations of Thymol Blue for the corrosion of C-steel after 120 min immersion in 1 M HCl at 25°C

Conc. x 10 ⁶ , M	θ	%IE
5	0.470	47.0
7	0.543	54.3
9	0.619	61.9
11	0.685	68.5
13	0.730	73.0
15	0.793	79.3

where $i_{\text{corr (free)}}$: represent the corrosion current density in the absence of inhibitor and $i_{\text{corr(inh)}}$: represents the corrosion current density in presence of inhibitor. Figure (2) indicated that by increasing the inhibitor concentration both cathodic and anodic current decreases with respect to the blank curve, which indicates a mixed type inhibitor is present [21-22], and we could expect that both anodic metal dissolution and cathodic H_2 reduction reactions rates are decreasing more by increasing the inhibitor concentration. Table (2) shows the obtained values of corrosion current density (i_{corr}), corrosion potential (E_{corr}), Tafel slopes (β_a and β_c), degree of surface coverage (θ) and inhibition efficiency (%IE) with the different concentrations of the investigated Thymol blue. The data provide in this Table indicate that the corrosion current density (i_{corr}) decreases with increasing the concentration of inhibitor while the values of β_a & β_c have very less deviation and almost parallel upon the addition of the investigated Thymol blue which indicates that Thymol blue doesn't change the corrosion mechanism [23] of the C-steel in 1 M HCl solution, but it blocks active metal sites for both anodic and cathodic processes. The small change of E_{corr} with increase of the concentration of

Thymol blue indicates that this compound is mixed type inhibitor.

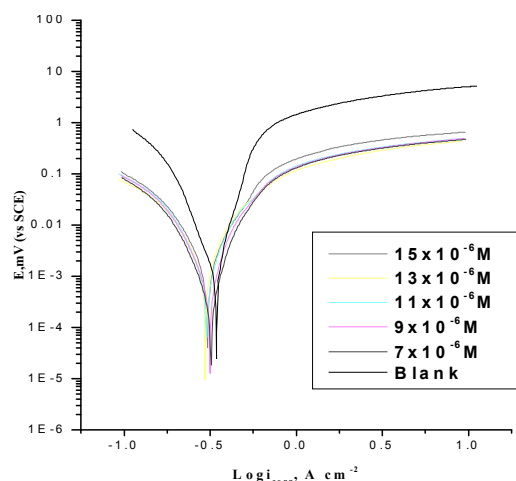


Figure 2. Potentiodynamic polarization curves for the dissolution of C- steel in 1 M HCl in the absence and presence of different concentrations of thymol blue at 25°C

Table (2): Effect of thymol blue concentrations on the free corrosion potential (E_{corr}), corrosion current density (i_{corr}), Tafel slopes (β_c , β_a), polarization resistance (R_p), corrosion rate (k_{corr}), degree of surface coverage (θ), and inhibition efficiency (%IE) of C- steel in 1 M of HCl at 25 C

Conc M	i_{corr} mA cm ⁻²	$-E_{\text{corr}}$ mV vs SCE	β_c mV dec ⁻¹	β_a mV dec ⁻¹	k_{corr} mmy ⁻¹	θ	%IE
Blank	16.8	462	154.8	100.7	767.5		
7×10^{-6}	14.3	516	182.8	160.2	651.9	0.148	14.8
9×10^{-6}	12.4	581	167.2	146.8	568.1	0.262	26.2
11×10^{-6}	7.59	521	141.1	120.0	347.0	0.548	54.8
13×10^{-6}	5.13	503	138.0	103.2	234.6	0.693	69.3
15×10^{-6}	2.78	496	123.8	92.8	126.8	0.835	83.5

3.3 Electrochemical impedance spectroscopy (EIS) measurements

The impedance diagrams are given in the Nyquist and Bode representations. The inhibition efficiency (%IE) and the surface coverage (θ) of the investigated inhibitor obtained from the impedance measurements can be calculated by applying the following relations:

$$\% \text{IE} = \theta \times 100 = [(R_{\text{ct}} - R_{\text{ct}}^0) / R_{\text{ct}}] \times 100 \quad (3)$$

Where R_{ct}^0 and R_{ct} are the charge transfer resistance in the absence and presence of the inhibitor, respectively

Figure (3a, b) shows EIS spectra in the form of a Nyquist diagram (a) and Bode (b) recorded on a C-steel electrode in 1 M HCl solution in the absence and presence of the investigated compound at different concentrations at 25°C. The Nyquist plots (a) showed that the diameter of the semicircle increases

with the increase in inhibitor concentration in the electrolyte, which indicating an increase in corrosion resistance of the material, the deviation from the perfect circular shape is related to heterogeneity due to the microscopic roughness of the electrode surface and inhibitor adsorption [24-25]. The capacitive loop at high frequencies represents the phenomenon associated with the double electric layer. It arises from the time constant of electrical double layer and the charge transfer in corrosion process [26]. The large capacitive loop makes an angle with the real axis and its intersection gives a resistance of the solution (R_s) enclosed between the working electrode and the counter electrode [27]. The presence of inductive loop may be attributed to the relaxation process obtained by adsorption species onto the electrode surface. The impedance spectra of the different Nyquist plots were analyzed by fitting the

experimental data to a simple equivalent circuit model as given in Figure (4) for C-steel, which includes the solution resistance R_s and the double layer capacitance C_{dl} which is placed in parallel to the charge transfer resistance R_{ct} [28] and C_{dl} is the constant phase element. The main parameters deduced from the analysis of Nyquist diagrams are: The resistance of charge transfer R_{ct} (diameter of high frequency loop) and the capacity of double layer C_{dl} which is defined as:

$$C_{dl} = \frac{1}{2\pi f_{max} R_{ct}} \tag{5}$$

where f is the maximum frequency. Table (3) is given the EIS data of C-steel in 1 M HCl with absence and presence of different concentrations of inhibitor at 25°C. The tabulated data indicate that by adding more of the investigated inhibitor R_{ct} values increase while C_{dl} values decrease, which refer to an increasing in thickness of electrical double layer which may corresponding with a decreasing in local dielectric constant, the higher R_{ct} value is indicating the lower corrosion state[29-30].

Table (3): EIS parameters for the corrosion of C-steel in 1 M HCl in the absence and presence of different concentrations of thymol blue at 25°C

Conc., M	R_{ct} Ω cm ²	C_{dl} , μ F cm ⁻²	θ	% IE
Blank	14.81	14.15	-----	-----
7×10^{-6}	18.554	12.89	0.201	20.1
9×10^{-6}	20.74	11.909	0.286	28.6
11×10^{-6}	23.23	9.212	0.362	36.2
13×10^{-6}	32.11	7.93	0.538	53.8
15×10^{-6}	64.77	4.23	0.771	77.1

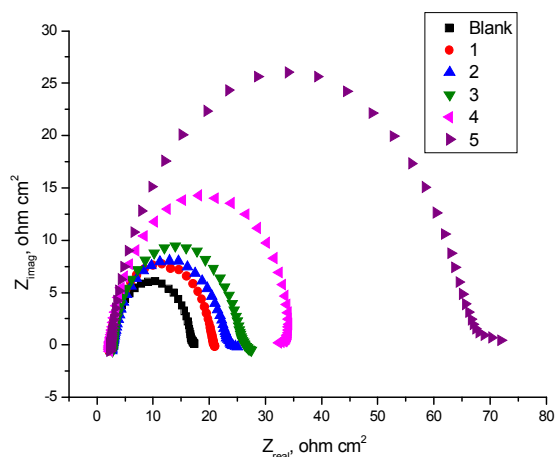


Figure 3a. The Nyquist plots for the corrosion of C-steel in 1 M HCl in the absence and presence of different concentrations of thymol blue at 25°C

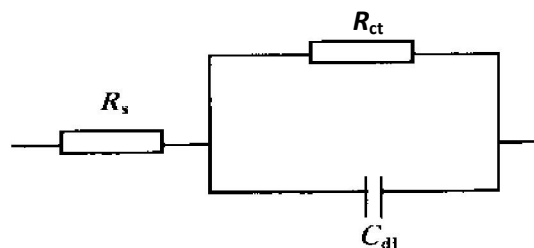


Figure 3b. Bode plots for the corrosion of C-steel in 1 M HCl in the absence and presence of different concentrations of thymol blue 25°C

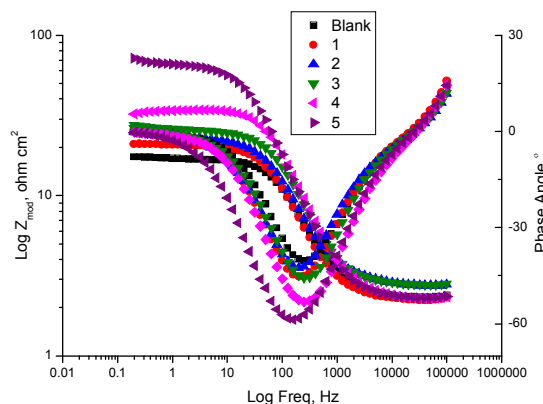


Figure (4): Equivalent circuit model used to fit experimental EIS data recorded for C-steel electrode in 1 M HCl

3.4 Electrochemical frequency modulation (EFM) measurements

Electrochemical frequency modulation (EFM) is a nondestructive technique that can directly and rapidly give values of the corrosion current without a prior knowledge of Tafel constants. Causality factor is considered to be its strength point as it serves as an internal check on the validity of the EFM measurements.[31,32]. With the electrochemical modulation technique (EFM), a potential perturbation by two sine waves of different frequencies is applied to the system. As a corrosion process is non-linear in nature, responses are generated at more frequencies than the frequencies of the applied signal. The current responses can be measured at zero, harmonic, and intermodulation frequencies. EFM 140 software was used to record the obtained EFM spectra. Analysis of these current responses can result in the corrosion current density and Tafel parameters. Inhibition efficiency and surface coverage can be determined using the relation (6):

$$\%IE = \theta \times 100 = [1 - (i_{corr(inh)} / i_{corr(free)})] \times 100 \tag{6}$$

where $i_{corr(free)}$ and $i_{corr(inh)}$ are the corrosion current densities in the absence and presence of inhibitor, respectively. Figure (7a, b) shows the EFM spectra for C-steel in 1 M HCl and in the presence 15×10^{-6} M

of at Thymol blue at 25°C. EFM results are spectrum of current that response as a function of frequency, the large peaks were used to calculate the corrosion current density (i_{corr}), Tafel slopes (β_c & β_a) and causality factors (CF-2 and CF-3) calculated values are given in Table (5). As shown from Table (5), the more the inhibitors concentration increase the less that i_{corr} value obtained, in other words the more we

add the investigated organic compounds we have less corrosion rate; we could easily notice that % IE values are increasing by increasing the Thymol blue concentration and the causality factors also indicate that the measured data are of good quality. We could also notice that the %IE values which obtained by EFM technique, EIS, polarization and weight loss are almost in the same range.

Table (4): Electrochemical kinetic parameters obtained from EFM technique for C-steel in 1 M HCl in the absence and presence of different concentrations of thymol blue

Conc M	i_{corr} $\mu\text{A cm}^2$	β_a mV dec^{-1}	β_c mV dec^{-1}	CF-2	CF-3	C.R. mmy^{-1}	θ	% IE
Blank	598.7	97	113	1.93	3.206	273.5		
7×10^{-6}	389.4	46	59	2.14	2.629	117.9	0.350	55.4
9×10^{-6}	330	40	43	2.23	2.972	150.9	0.449	81.6
11×10^{-6}	295.9	34	37	1.92	2.882	135.2	0.506	50.6
13×10^{-6}	267.2	87	97	2.019	2.957	122.1	0.554	55.4
15×10^{-6}	110.2	63	75	2.089	3.15	50.37	0.816	81.6

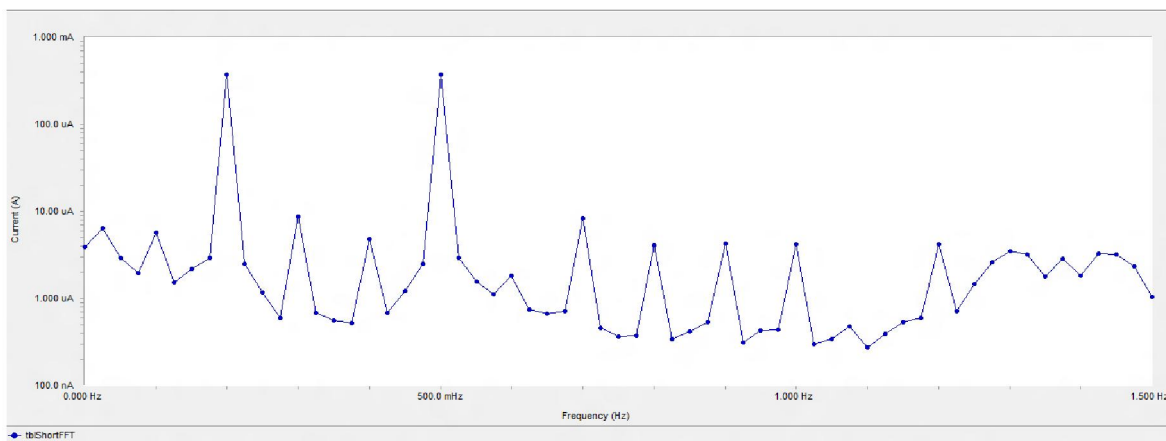


Figure (5a): EFM spectra for C-steel in 1 M HCl (Blank) in absence of Thymol blue

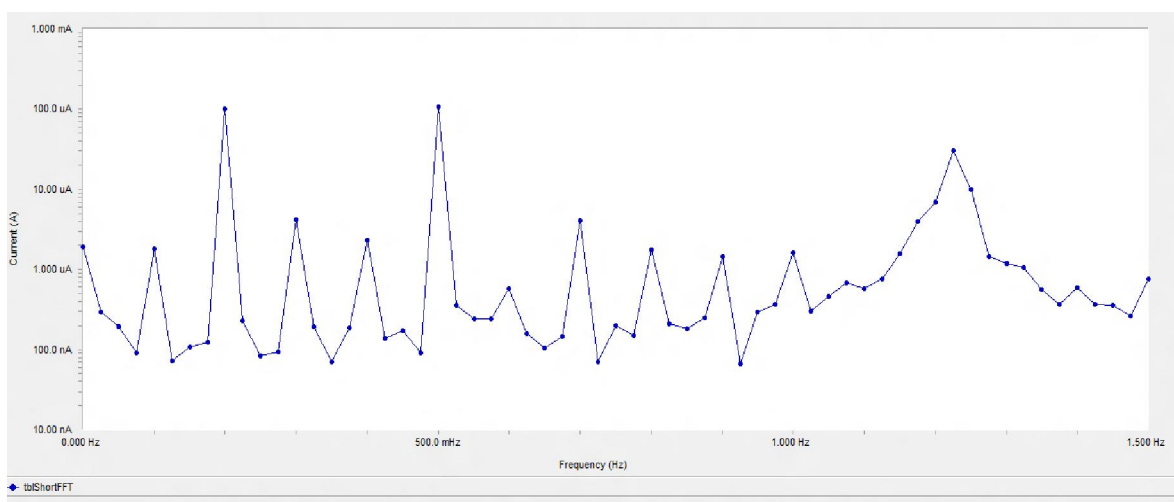


Figure (5b): EFM spectra for C-steel in 1 M HCl in presence of 15×10^{-6} M of Thymol blue

3.5 Scanning electron microscopy (SEM) studies

Figure (6) contain 2 different SEM micrographs of C-steel samples. First sample Fig (6a,b) showing the surface of the C-steel alone with no any addition of inhibitor or electrolyte, Fig 6b showing the C-steel surface in the presence of the 1 M HCl only with no any addition of inhibitor blank, while Figure 6c represents the SEM micrographs of C-steel in presence of 1 M HCl and 15×10^{-6} M of Thymol Blue. We could notice that in Figure 6b it is clearly shown the formation of pits, cracks and corrosion products in C- steel surface, while in Figure 8c it minimized with the presence of the 15×10^{-6} M of Thymol blue, also the smoother surface in the Figure 6c indicating the adsorbing of the previous noticed inhibitor on the C-steel metal to form a passive layer which will block the active sites on the C-steel surface leading to decrease the rate of corrosion. Or due to the involvement of inhibitor molecules in the interaction with the reaction sites of C-steelalloy surface, resulting in a decrease in the contact between C-steelalloy and the aggressive medium and sequentially exhibited excellent inhibition effect [33].

3.6 Energy dispersive X-ray spectroscopy (EDX) studies

EDX is using to determine the elements present on the surface of the metal such data will help to stimulate what happening on the surface of the metal in case of absence and the presence of electrolyte and inhibitor, Figure (7) shows 4 different spectra of EDX of C-steel samples (a, b,c) First sample Fig (9a) showing the surface of the C-Steel alone with no any addition of inhibitors or electrolyte, Fig (20 B) showing the C-steel surface in the presence of the 1 M HCl only with no any addition of inhibitor, while Figure 7c represents the SEM micrographs of C-steel in presence of 1 M HCl and 15×10^{-6} M of Thymol blue. Through the Figure 7c we could obtain additional lines indicating more C, S, O than in case of Figure 7 a, b which indicating the presence of the investigated Organic compounds on the surface of the C-steel. Exact analyzed details are given in Table (5).

Through the analyzed data it become clear that in case of blank “absence of the investigated organic compounds “there is presence of C, O which indicates that the surface of the metal is covered with the Fe_2O_3 layer, while in case of additional of the investigated organic compounds we could obtain that (C, S, O) values increase which indicating the adsorbing of the inhibitors on active sites of the surface of C-steel.

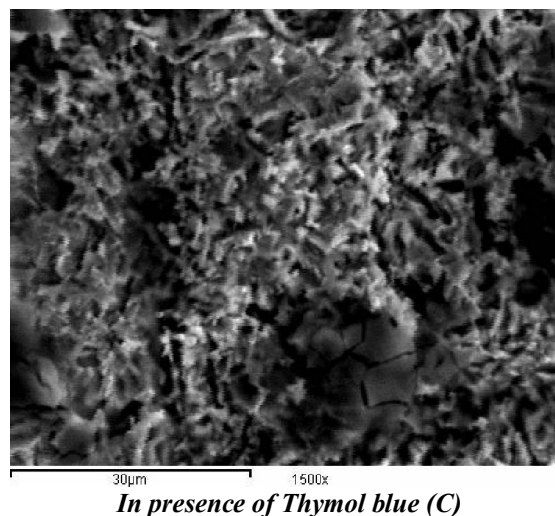
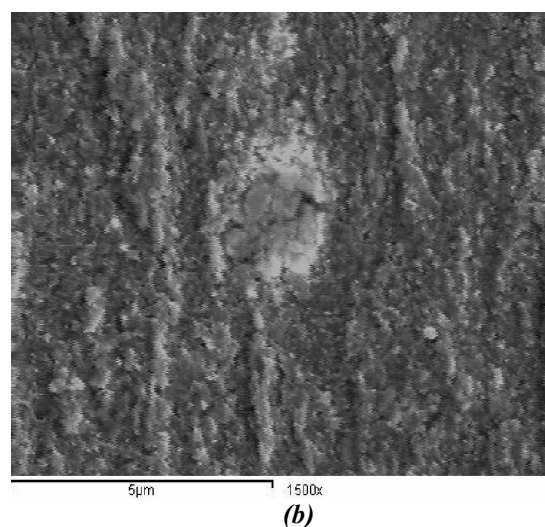
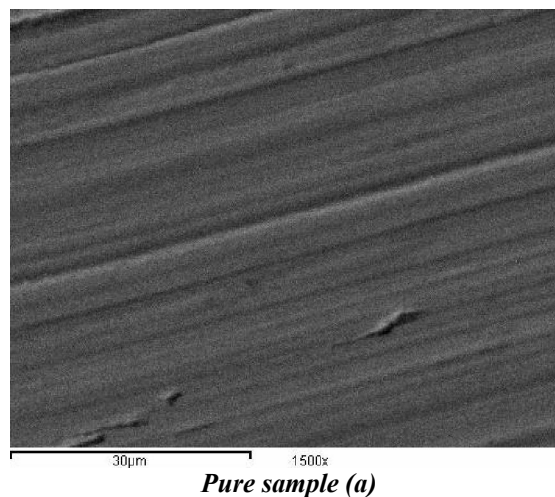
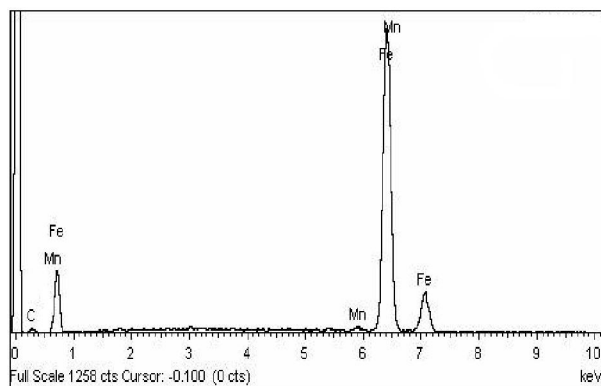
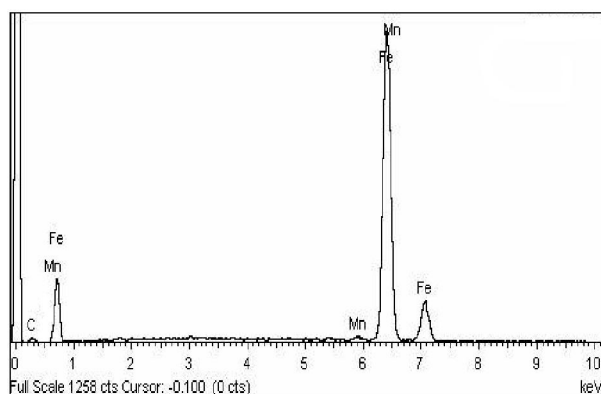
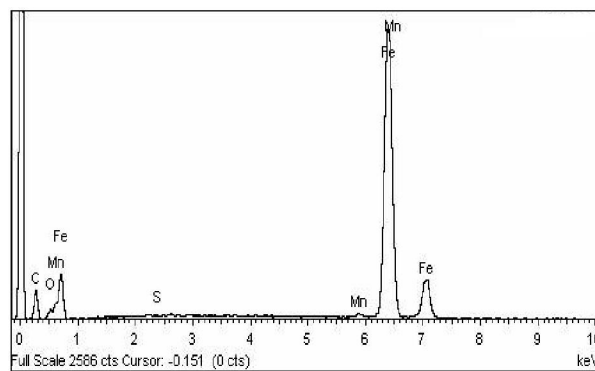


Figure (6) shows themicrographs of C-steel samples in present and absence of Thymol blue

**Pure sample (a)****Blank (b)****Immersed in Thymol Blue (C)****Figure 7.** Show themicrographs of C-steel samples in present and absence of Thymol blue

3.7. Adsorption Isotherms

As discussed in the previous results, the investigated compounds show similar characteristics as most of organic inhibitor to be adsorb on to the metal surface and form a protective film, thus the studying of the adsorption isotherm would be very valuable as it would provide data to understand more the nature of the metal- inhibitor interaction. A number of mathematical relationships for the adsorption were applied. The experimental data give good curves fitting for the applied adsorption isotherm as the correlation coefficients (R^2) were in the range 0.980-0.997 shown in Figure8. The Langmuir isotherm:

$$(\theta/1-\theta) = KC \quad (7)$$

Table (5): Surface composition (weight %) of C-steel after 3 days of 3 days of immersion in a 1 M HCl solution in the absence of the investigated Thymol blue

(Mass %)	Fe	Mn	C	O	N	Cl	S	Br
Fresh sample	95.43	0.63	3.94	-	-	-	-	-
Blank	65.45	0.57	3.32	30.15	-	0.51	-	-
Thymol Blue	62.72	0.54	20.87	13.96	-	-	1.91	-

Where θ is the surface coverage, K is equilibrium constant of adsorption process, C is concentration of inhibitor. The equilibrium constant of adsorption can be related to the free energy change (ΔG_{ads}°) by the following relation:

$$K_{eqm} = 1/55.5 \exp -\Delta G_{ads}^\circ/RT \quad (8)$$

where R is the universal gas constant, T is the absolute temperature, 55.5 is referring to the water concentration in solution in mol L^{-1} . The data recorded in Table 6 indicate that the adsorption of the investigated compound on the surface of C-steel surface is spontaneous process as the ΔG_{ads}° values have negative values[34-35]. The values of K were found to run parallel to the %IE Thymol blue. This result reflects the increasing capability due to structural formation on the metal surface [36]. To obtain the values of, ΔH_{ads}° and ΔS_{ads}° a plot between

$\log K_{ads}$ and $1/T$ was done shown in Figure (9) slope would be equal to the value ($-\Delta H_{ads}^\circ/R$) according to the following equation [37] of van't Hoff:

$$\log K_{ads} = (-\Delta H_{ads}^\circ / 2.303RT) + \text{constant} \quad (9)$$

By obtaining the, ΔH_{ads}° value, the following equation [38] would be useful to obtain the values of, ΔS_{ads}° all estimated thermodynamic adsorption parameters for the studied compounds on carbon steel from 1M HCl solution were listed in Tables (6).

$$\Delta G_{ads}^\circ = \Delta H_{ads}^\circ - T\Delta S_{ads}^\circ \quad (10)$$

It is usually accepted that the value of ΔG_{ads}° around -20 kJ mol^{-1} or lower indicates the electrostatic interaction between charged metal surface and charged organic molecules in the bulk of the solution while those around -40 kJ mol^{-1} or higher involve charge sharing or charge transfer between the metal surface and organic molecules [39]. From the

obtained values of ΔG°_{ads} it was found the existence of comprehensive adsorption (physical and chemical adsorption). In this processes, the covalent bond is formed by the charge sharing or transferring from the inhibitor molecules to the metal surface [40-41], while the negative values of the ΔH°_{ads} referring to the adsorption of the investigated compounds on the surface of the metal are exothermic processes [42-43] the values of ΔS°_{ads} in the presence of the investigated compounds are large and negative as accompanied with exothermic adsorption processes.[44]

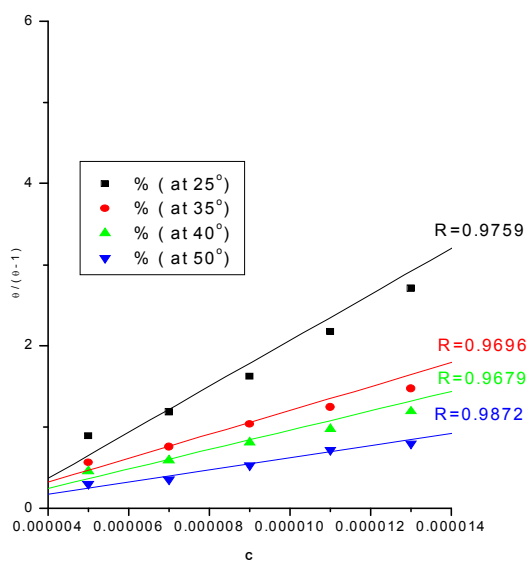


Figure (8): Langmuir adsorption isotherm of Thymol blue on C-steel surface in 1 M HCl at different temperatures

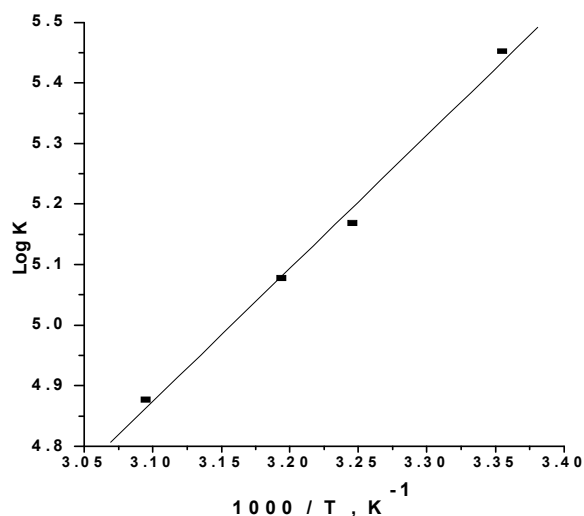


Figure (9): (log K) vs. (1/T) for the corrosion of C-steel in 1 M HCl in the presence of Thymol blue

3.8. Effect of temperature

To study the effect of temperature on the rate of the corrosion toward C-steel in 1 M HCl in presence of The investigated compounds, the weight loss results which done in temperature range from 25 to 50 °C were used, the results indicates that the corrosion rate increases due to increasing of the temperature and decreases with the increasing of Thymol blue concentration, to calculate the activation energy (E_a^*) Arrhenius equation was used:

$$k_{corr} = A \exp(-E_a^*/RT) \quad (11)$$

where k_{corr} is the rate of corrosion and A is the Arrhenius constant. Values of activation energy E_a^* obtained by plotting $\log k_{corr}$ versus $1/T$ gave straight lines as shown in Figure 10. Transition state theory were used to calculate the values of (ΔH^* , ΔS^*) through the following equation

$$k_{corr} = (RT/Nh) \exp(\Delta S^*/R) \exp(-\Delta H^*/RT) \quad (12)$$

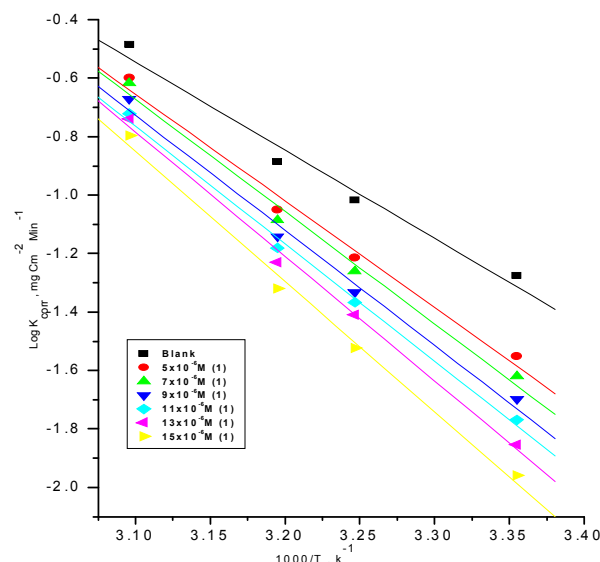


Figure10: Arrhenius plots for C-steel corrosion rates (k_{corr}) after 120 min of immersion in 1 M HCl in the absence and presence of various concentrations of Thymol blue

where h is Planck's constant and N is Avogadro's number. Figure 11 shows a plot of (Rate/T) vs. $1/T$ for C-steel in 1 M HCl at different concentrations of investigated compounds as shown in the plot the linear coefficient (R^2) values are close to 1, the calculated values of E_a^* , ΔH^* and ΔS^* are given in Table 7. The tabulated data indicated a strong adsorption for the investigated compounds on the surface of the metal, E_a^* values were increase more by increasing the concentrations of the used inhibitor,

therefore, we can conclude that the presence of this compound induce an energy barrier for the corrosion reaction and this barrier increases with increasing the concentration of Thymol blue. The positive signs of ΔH^* reflect the endothermic nature of the steel dissolution process and the increasing of this values indicates the presence of an energy barrier for the corrosion process due to the existence of these additives i.e., the process of adsorption exhibits a rise in the enthalpy of the corrosion process. The entropy of activation (ΔS^*) in the absence and presence of inhibitors has negative values. This indicates that the activated complex in the rate determining step represents an association rather than dissociation, meaning that, a decrease in disordering takes place on going from reactants to the activated complex [45].

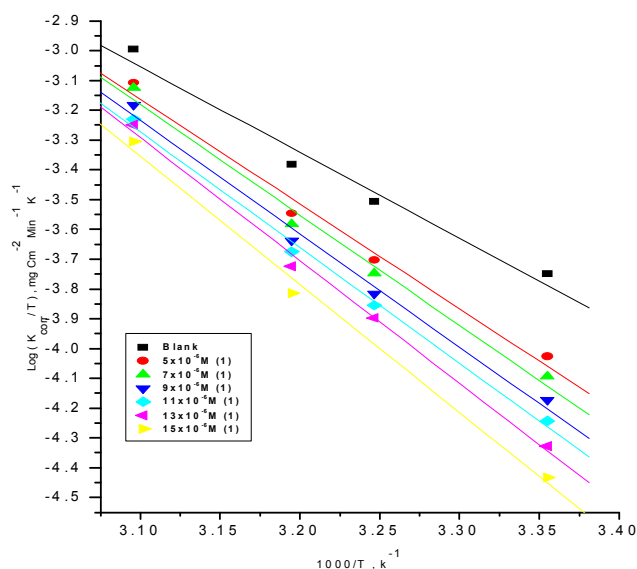


Figure (11): Transition-state for C-steel corrosion rates (k_{corr}) in 1 M HCl in the absence and presence of various concentrations of Thymol blue

3.9. Mechanism of corrosion inhibition

The obtained data of weight loss and electrochemical methods gave approximately the same values of inhibition efficiency and indicate that by increasing the concentration of the investigated compound the inhibition efficiency increases. The essential effect of this compound as corrosion inhibitor is due to the presence of free electron pairs on the oxygen and sulfur atoms, π -electrons on the aromatic rings, molecular size, heat of hydrogenation and mode of interaction with the metal surface [46-47]. C-steel has co-ordination affinity towards O and S bearing ligands [48-49]. Hence, adsorption on C-steel can be attributed to co-ordination through hetero-atoms and π -electrons of aromatic rings. Another striking feature for high inhibition

performance of the studied compound is the presence of S-atom. The presence of S-atom in the inhibitor structure makes the formation of $d\pi-d\pi$ bond resulting from overlap of 3d-electrons from C-steel atom the 3d vacant orbital of S-atom possible, which enhances the adsorption of the compounds on the metal surface. Thymol blue gives higher inhibition efficiency value, as it contains (3O, 1S atoms) and relatively higher molecular weight. This indicates the effect of the presence of S atom which enhances the delocalized π -electrons on the active centers of the compound.

References

1. Proceedings of 1st to 8th European symposium on corrosion inhibitors every 5 years held in Ferrara.
2. M.Elachouri, M R. Infante, F.Izquierdo, S. Kertit, H.M>Gouttoya, B Nicricorros. Sci, 43 (2001) 19-35.
3. D. Chebabe, Z. AitChikh, N- Hajjaji A Srhiri, F. Zucchi, Corros. Sci 45 (2003) 409-320.
4. N. Hajjaji, I. Rico, A.srhiri, A. Lattes, M. Soufiaoui A Ben Bachir, Corros. Sci, 49 (4) (1993) 326-334.
5. J. M. Bastidas, J.L.Polo, E.cano, J. Appl. Electrochem 30 (2000) 1173-1177.
6. N.E Hamner, In: C.C. Nathan (ed.) corrosion inhibitor, Nace Houston, Texas, USA 1973. P.I.
7. M. Elachouri, M.S. Hajji, s. Kertit, E.M. Essasi, M Salem, R. Coudert, Corros. Sci. 37(1995) 381.
8. B. Mernari, H. Elattari, M. Traisnel, F. Bentiss, M. Lagrenee, Corros. Sci 40 (1998)391.
9. F. Zucchi, G. Trabanelli, G. Brunoro, Corros. SCI.36 (1994) 1683.
10. Cizekmater perform. 33(1994) 56.
11. W.W Frenier, F.B. Grow Cock, In: A. Raman, P. Labine (Eds), Review on corrosion science and technology, NACE international Houston, Tx 1993, PP. 11- 201.
12. S. Muralidharan, K.L.N phani, S,Pitchuani, S Ravichandran, S.V.K. Leyer, J. Electrochem. SOC 142 (1995)1478.
13. N. Hackerman, R.M. hurd, In: proceeding of the international congress of metallic corrosion, Butterworth London, 1962, P.166.
14. Raj Narayan; An Introduction to Metallic Corrosion and its Prevention; Oxford and IBH publishing Co. Pvt. Ltd., (1998).
15. G.N., Mu, T.P., Zhao, M., Liu, T., Gu, (1996) Effect of Metallic Cations on Corrosion Inhibition of an Anionic Surfactant for Mild Steel ,Corrosion 52, 853.

16. V. Otieno-Alego, G. A. Hope, H.J. Flitt, G. A. Cash and D. P. Schweinberg, *Corros. Sci.*, 33 (1992) 1719.
17. M.Sahin, S.Bilgic and H. Ylmaz, *Appl. Surf. Sci.* 195 (2002) 1.
18. R.G., Parr, D.A., Donnelly, M., Levy, M., Palke, (1978): Electronegativity: The density functional viewpoint, *J. Chem. Phys.* 68,3801-3807.
19. F. Bentiss, M. Lagrenee, M. Traisnel, 2,5-Bis(n-pyridyl)-1,3,4-oxadiazoles as corrosion inhibitors for mild steel in acidic media, *Corrosion* 56 (2000) 733.
20. S. Omanovic, S.G. Roscoe, Effect of linoleat on electrochemical behavior of stainless steel in phosphate buffer, *Corrosion* 56 (2000) 684.
21. J., Aljourani, K., Raeissi, M.A., Golozar, (2009): Benzimidazole and its derivatives as corrosion inhibitors for mild steel in 1M HCl solution, *Corros. Sci.*, 51,1836.
22. H., Amar, A., Tounsi, A., Makayssi, A., Derja, J., Benzakour, A., Outzourhit, (2007) Corrosion inhibition of Armco iron by 2-mercaptobenzimidazole in sodium chloride 3% media *Corros. Sci.*,49, 2936.
23. T.P. Hoar, R.P. Khera, *Proceedings 1st EuropSymp. on Corrosion Inhibitors, Ferrara, Italy, 1960.* 73.
24. C.C. Nathan, *Corr.* 9(1959)199.
25. N. Hackerman and K. Amarak, *J. Electrochem. Soc.*, 115(1982) 1007.
26. S. S. Abd El-Rehim, H. H. Hassan and M. A. Amin, *Mater. Chem. Phys.* 70 (2001) 64.
27. K. F. Khaled and M. M. Al-Qahtani, *Mater. Chem. Phys.* 113 (2009) 150.
28. C. Jeyaprobha, S. Sathiyarayanan and G. Venkatachari, *Appl. Surf. Sci.* 253 (2006) 423.
29. R.B. Mathur and T. Vasudevan, *Corr.* 38(3) (1982) 171.
30. F. Mansfeld and Y.J. Lorenz, *Corr. Sci.*, 21(9) (1981) 647.
31. X. Li, S. Deng, H. Fu and T. Li, *Electrochim. Acta*, 54 (2009) 89.
32. T. Paskosy; *J. Electroanal.Chem.* 364 (1994) 111.
33. R.A. Prabhu, T.V.Venkatesha, A.V.Shanbhag, G. M. Kulkarni, R.G.Kalkhambkar, *Corros. Sci.*, 50 (2008) 3356.
34. A.El-Awady, B. Abd El-Nabey and S. G. Aziz, *Electrochem. Soc.* 139 (1992) 2149.
35. Singh, A., Chaudhary, R. S., *Br. Corros. J.* 31(4) (1996), 300,511.
36. S. L. F. A. Da Costa and S. M. L. Agostinho, *Corrosion*, 45 (1989) 472.
37. Popova, E. Sokolova, S. Raicheva and M. Christov, *Corros. Sci.* 45 (2003) 33.
38. E. Khamis, *Corrosion (NACE)* 46 (1990) 476.
39. S. S. Abd El-Rehim, H. H. Hassan and M. A. Amin, *Mater. Chem. Phys.* 70 (2001) 64.
40. Z. Szlarska-Smialowska, *Corros. Sci.* 18 (1978) 953.
41. Yurt, S. Ulutas, H. Dal, *Appl. Surf. Sci.* 253 (2006) 919.
42. L. Tang, X. Lie, Y. Si, G. Mu and G. Liu, *Mater. Chem. Phys.* 95 (2006) 29.
43. L. Tang, G. Murad and G. Liu, *Corros. Sci.* 45 (2003) 2251.
44. X. Li and L. Tang, *Mater. Chem. Phys.* 90 (2005) 286.
45. X. Li and G. Mu, *Appl. Surf. Sci.* 252 (2005) 1254.
46. M. I. Awad, *J. of Appl. Electrochem.*, 36, 10, (2006) 1163.
47. S. R. Sainkar, V. Shinde, S. A. Gangal and P. P. Patil, *J. Mater. Sci.*, 41, 10 (2006) 2852.
48. M. Ehteshamzadeh, T. Shahrabi and M. Hosseini, *Anti- Corros. Methods & Mater.*, 53, 13 (2006) 147.
49. S. Sriram, R. Balasubramaniam, M. N. Mungole, S. Bharagava and R. G. Baligheid, *Corros. Sci.*, 48 (2006) 1059.